

## RAPID COMMUNICATION

*In vivo* detection of brain Krebs cycle intermediate by hyperpolarized magnetic resonanceMor Mishkovsky<sup>1,2</sup>, Arnaud Comment<sup>3</sup> and Rolf Gruetter<sup>1,2,4</sup>

The Krebs (or tricarboxylic acid (TCA)) cycle has a central role in the regulation of brain energy regulation and metabolism, yet brain TCA cycle intermediates have never been directly detected *in vivo*. This study reports the first direct *in vivo* observation of a TCA cycle intermediate in intact brain, namely, 2-oxoglutarate, a key biomolecule connecting metabolism to neuronal activity. Our observation reveals important information about *in vivo* biochemical processes hitherto considered undetectable. In particular, it provides direct evidence that transport across the inner mitochondria membrane is rate limiting in the brain. The hyperpolarized magnetic resonance protocol designed for this study opens the way to direct and real-time studies of TCA cycle kinetics.

*Journal of Cerebral Blood Flow & Metabolism* (2012) **32**, 2108–2113; doi:10.1038/jcbfm.2012.136; published online 19 September 2012

**Keywords:** acetate; dynamic nuclear polarization; hyperpolarization; real-time metabolism; TCA cycle; 2-oxoglutarate

## INTRODUCTION

The connection between cerebral energy metabolism and neural function was highlighted more than a century ago.<sup>1</sup> Following Krebs' formulation, it became well established that the tricarboxylic acid (TCA) cycle is central to brain energy homeostasis,<sup>2</sup> as it is the final common path for aerobic oxidation of any molecule that can be transformed into an acetyl group (carbohydrates, fatty acids, and amino acids). In addition, the cycle serves as a source of biosynthetic precursors for synthesis of physiological amino acids. Several crucial questions are, however, left unanswered, in particular the regulation of the metabolism of glutamate (Glu), the major excitatory neurotransmitter. Glutamate is in dynamic exchange with the TCA cycle intermediate 2-oxoglutarate (2OG; IUPAC nomenclature for  $\alpha$ -ketoglutarate) through reactions that are key to the regulation of cellular oxygen metabolism such as the malate-aspartate shuttle, aspartate aminotransferase (AAT), and glutamate dehydrogenase. A difficulty in addressing the regulation of TCA cycle activity *in vivo* is rooted in the fact that the concentrations of TCA cycle intermediates are too small to be detectable using established *in vivo* methods such as magnetic resonance (MR).<sup>3</sup> To date, TCA cycle activity *in vivo* has been exclusively studied using carbon-13 (<sup>13</sup>C) magnetic resonance spectroscopy (MRS), a technique that enables the investigation of metabolic processes *in vivo* in a non-invasive manner.<sup>4</sup> Because of the <sup>13</sup>C low natural abundance of ~1%, this type of experiment requires the infusion of a suitable <sup>13</sup>C-labeled precursor, which leads to the distribution of the <sup>13</sup>C-label among the metabolic products and allows probing specific pathways.<sup>5–7</sup> The turnover of the label from precursors to products is typically measured from the time course of <sup>13</sup>C concentration changes readily quantifiable from the <sup>13</sup>C MR spectrum of the many available precursors.

<sup>13</sup>C-labeled acetate has been used to investigate the TCA cycle rates using MRS. Acetate has the advantage of being readily taken up by the brain and as it is solely metabolized in astrocytes, it has been used as a tracer to study glial metabolism *in vivo* in rats<sup>8–10</sup> and in humans.<sup>11</sup> However, most of the molecules that become labeled as a consequence of the acetate infusion cannot be detected by MR *in vivo* because of their low concentration and the relatively low sensitivity of *in vivo* MR. Only the most concentrated amino acids, e.g., Glu, glutamine, and aspartate can be detected *in vivo*.<sup>3–5,12</sup> These amino acids are not part of the TCA cycle but indirectly reflect TCA cycle activity because of label incorporation from TCA cycle intermediates, namely, 2OG and oxaloacetate. The assumption required for determining TCA cycle flux through <sup>13</sup>C isotopomer analysis is that the relative concentration of <sup>13</sup>C isotopomers is identical in precursors and their detectable metabolic products.<sup>13</sup> In addition, dynamical analysis through this method is only representative of the TCA cycle kinetics if the exchange rate between TCA intermediates and products is at least on the same order of magnitude as the TCA cycle flux. Therefore, the direct detection of TCA cycle intermediates would provide new crucial information concerning the kinetics of the label flow through the TCA cycle.

## MATERIALS AND METHODS

Dynamic Nuclear Polarization of <sup>13</sup>C-labeled Acetate

The <sup>13</sup>C nuclear spins in frozen glassy solutions of sodium [1-<sup>13</sup>C]acetate or sodium [1,2-<sup>13</sup>C<sub>2</sub>]acetate (Sigma-Aldrich, Buchs, Switzerland) were dynamically polarized using a custom-designed DNP polarizer operating at 5 T and 1 ± 0.05 K as described in earlier publications.<sup>14,15</sup> A 4.5 mol/L solution of sodium [1-<sup>13</sup>C]acetate or sodium [1,2-<sup>13</sup>C<sub>2</sub>]acetate dissolved in a

<sup>1</sup>Laboratory for Functional and Metabolic Imaging, Ecole Polytechnique Fédérale de Lausanne, Lausanne, Switzerland; <sup>2</sup>Department of Radiology, University of Lausanne, Lausanne, Switzerland; <sup>3</sup>Institute of Physics of Biological Systems, Ecole Polytechnique Fédérale de Lausanne, Lausanne, Switzerland and <sup>4</sup>Department of Radiology, Geneva University Hospital and Faculty of Medicine, University of Geneva, Geneva, Switzerland. Correspondence: Professor A Comment, Institute of Physics of Biological Systems, Ecole Polytechnique Fédérale de Lausanne, EPFL SB IPSB GR-CO, Station 6, Lausanne CH-1015, Switzerland. E-mail: arnaud.comment@epfl.ch

This work was supported by the Swiss National Science Foundation (grants 200020\_124901 and PP00P2\_133562 to A.C. and grant 31003A\_131087 to R.G.), the National Competence Center in Biomedical Imaging, the Centre d'Imagerie BioMédicale of the UNIL, UNIGE, HUG, CHUV, EPFL, and the Leenards and Jeantet Foundations.

Received 13 March 2012; revised 2 August 2012; accepted 23 August 2012; published online 19 September 2012

2/1 (vol/vol) D<sub>2</sub>O/d<sub>6</sub>-ethanol (Cambridge Isotope Laboratories, Andover, MA, USA) containing 33 mmol/L of TEMPO nitroxyl radical (2,2,6,6-tetramethyl-1-piperidinyloxy, Sigma-Aldrich) was prepared. Droplets of solution were plunged in liquid nitrogen to form frozen beads of ~2 mm diameter. A volume of 0.4 ml of frozen solution was placed inside the DNP polarizer sample holder, which was then inserted into the microwave cavity located within the cryostat filled with ~0.5 L of liquid helium at atmospheric pressure (4.2 K). The vacuum pump system was then turned on to lower the temperature of the sample space such as to maintain the frozen sample under superfluid helium at 1 ± 0.05 K.

The microwave power at the output of the source was set to 40 mW and the irradiation frequency was set to 139.85 GHz. The nuclear polarization was monitored as a function of time by means of pulsed nuclear magnetic resonance using 5° tipping pulses. Once the polarization of the <sup>13</sup>C nuclei had reached a targeted value (the <sup>13</sup>C solid-state polarization reached 12 ± 2% after 2 ± 0.4 hours in sodium [1-<sup>13</sup>C]acetate samples and after 1 ± 0.2 hours in sodium [1,2-<sup>13</sup>C<sub>2</sub>]acetate samples), the frozen solution was dissolved in 5 ml of superheated D<sub>2</sub>O (170 °C) by means of a dissolution apparatus similar to the one described by Ardenkjaer-Larsen *et al.*<sup>16</sup> In the system used for the present study, a helium gas stream drove the resulting solution out of the polarizer magnet through a 5-m long capillary into the bore of an animal imager, where the sample was collected in a remotely controlled infusion pump that separated the liquid solution from the gas, and infused a chosen amount of liquid solution into an animal.<sup>14</sup> Note that the solution contained a residual 2 mmol/L TEMPO radical, but its effect on acetate <sup>13</sup>C *T*<sub>1</sub> is negligible.<sup>17</sup> The delay between dissolution and infusion was set to 3 seconds.

#### Animal Preparation

All animal experiments were conducted according to federal and local ethical guidelines, and the protocols were approved by the local regulatory body of the Canton Vaud, Switzerland (Service de la consommation et des affaires vétérinaires, Affaires vétérinaires, Canton de Vaud, Suisse).

*In vivo* experiments were performed on male Sprague–Dawley rats (~450 g). Animals were anesthetized with 1.5% isoflurane in a 30% O<sub>2</sub>/70% N<sub>2</sub>O mixture. A femoral vein was catheterized for acetate infusion. The rat was placed on a holder along with the infusion pump and the femoral vein catheter was connected to the outlet of the pump. The holder was then inserted inside the scanner. A bolus of ~2.2 ml of hyperpolarized solution containing ~0.3 mol/L of the <sup>13</sup>C-labeled acetate was infused within 9 seconds. It contained a residual TEMPO concentration of ~2 mmol/L and 2% of deuterated ethanol. Such concentrations should not affect cerebral metabolism within the time frame of our experiments. As mentioned by Sano *et al.*,<sup>18</sup> most commercially available nitroxyl radicals are water-soluble and cannot pass through the blood–brain barrier. It was also showed in a recent *in vivo* <sup>13</sup>C MRS study that the cerebral metabolism observed after the infusion of [1-<sup>13</sup>C]ethanol in rats at an ~10-fold higher concentration than used in the present study is very similar to the metabolism observed after the injection of [1-<sup>13</sup>C]acetate as a consequence of the conversion of ethanol to acetate in the liver and subsequent recirculation of acetate into the brain.<sup>19</sup> In our study, only ~1% of the <sup>13</sup>C's come from residual ethanol. Rat physiology was monitored during the experiments: body temperature was kept between 37 °C and 38 °C while respiration rate was maintained at 60 per min by adjusting the isoflurane level in respiratory gases. The rate and dose of the infusion was determined in bench experiments to insure that the bolus-like infusion is not lethal for rats. The blood volume for a 450-g rat is ~28 mL.<sup>20</sup> Taking into account that sodium concentration in the blood is ~150 mmol/L, a bolus injection of 2.2 mL with a concentration of 300 mmol/L of sodium acetate will lead to a sodium plasma concentration of ~160 mmol/L further attenuated during the time course by exchange with interstitial fluid. As the recorded physiological parameters (temperature, respiration rate as well as blood pH during the preparatory experiments) were stable throughout the experiments, we considered that this modest temporary increase in Na<sup>+</sup> concentration had no influence on animal physiology. As shown by Lien *et al.*,<sup>21</sup> no variations in brain metabolite concentrations such as Glu concentration were observed within 2 hours of acute hypernatremia (serum sodium 194 ± 5 mmol/L). We do not expect that any change can occur within a minute after the injection of the bolus. At the end of the experiment, animals were killed with an overdose of pentobarbital.

#### Magnetic Resonance Imaging and MRS Experiments

All measurements were performed on a Varian INOVA spectrometer (Varian, Palo Alto, CA, USA) interfaced to a 31-cm horizontal-bore actively

shielded 9.4 T magnet (MagneX Scientific, Abingdon, UK). Radiofrequency (RF) transmission and reception was done using a home-built hybrid surface coil consisting of a proton quadrature coil and a three-loop 10-mm diameter carbon coil. This coil was placed on top of the rat head. The <sup>13</sup>C spectra were acquired through single-pulse experiments with 30° BIR-4 adiabatic radiofrequency pulses to compensate for B<sub>1</sub> inhomogeneities.<sup>22</sup> Localization was achieved using an outer volume suppression scheme<sup>23</sup> with voxels volume of 343 μL (7.3 × 9.4 × 5 mm<sup>3</sup>). The time course measurements were acquired in a voxel of 275 μL (5 × 5 × 5 mm<sup>3</sup>) using a series of 30° pulse applied every 3 seconds. The acquisition time was set to 200 ms. To generate an external reference signal, a small sphere filled with 99% <sup>13</sup>C-labeled formic acid was placed in the center of the carbon coil. High-order shimming was performed using the FASTESTMAP algorithm.<sup>24</sup> Data were processed using MATLAB. To perform homonuclear polarization transfer between the two <sup>13</sup>C spins of acetate, we used a specific pulse sequence consisting of a single-voxel localization scheme (7.3 × 9.4 × 5 mm<sup>3</sup>) followed by three 90° radiofrequency pulses.<sup>25</sup>

#### RESULTS

Dissolution dynamic nuclear polarization (dissolution DNP),<sup>16</sup> a hyperpolarization technique based on low-temperature microwave-driven polarization transfer from the electron spins of paramagnetic centers to precursors nuclear spins<sup>26</sup> and providing an increase in MR sensitivity of up to four orders of magnitude, was implemented as follows: low-temperature DNP was performed in superfluid helium at 1 ± 0.05 K using a home-built 5 T polarizer coupled to a 9.4-T animal scanner<sup>14,15</sup> and, 3 seconds after dissolution, <sup>13</sup>C-labeled hyperpolarized acetate (<sup>13</sup>C polarization of 12 ± 2%) was injected in the rats femoral vein before MRS measurements. The hyperpolarized <sup>13</sup>C signal was detectable over a time period on the order of the characteristic time *T*<sub>1</sub> required for the spin magnetization to return to its thermal equilibrium value. The *in vivo* <sup>13</sup>C characteristic signal decay time after bolus injection of the hyperpolarized [1-<sup>13</sup>C]acetate solution was deduced by fitting the signal amplitude (corrected for the effect of the radiofrequency pulses) with a decaying mono-exponential function and was determined to be 15 ± 2 seconds in the rat head (*n* = 4; data not shown).

To selectively measure the <sup>13</sup>C signal from the brain, a localization pulse sequence was used in conjunction with a surface coil.<sup>23</sup> A <sup>13</sup>C spectrum observed in the brain 16 seconds after dissolution (Figures 1A and 1B) delineates two peaks separated by 0.15 p.p.m., which were detected in all animals (*n* = 3). The more intense signal (182.2 p.p.m.) was unambiguously assigned to the carboxyl <sup>13</sup>C of the injected acetate molecule.<sup>27</sup> The less intense resonance at 182.05 p.p.m. likely originated from a metabolic product of acetate. The chemical shift of 182.05 p.p.m. is within 8 Hz of the reported *in vitro* value of the 5-<sup>13</sup>C resonance of [5-<sup>13</sup>C]2OG.<sup>27</sup> Observing the incorporation of [1-<sup>13</sup>C]acetate into [5-<sup>13</sup>C]2OG should imply, considering the well-established metabolic pathways of acetyl-CoA metabolism in the TCA cycle, that the creation of [4,5-<sup>13</sup>C<sub>2</sub>]2OG from [1,2-<sup>13</sup>C<sub>2</sub>]acetyl-CoA is detectable. Therefore, a second set of experiments (*n* = 3) was performed under identical conditions, except that [1,2-<sup>13</sup>C<sub>2</sub>]acetate was infused. The interaction between the two adjacent <sup>13</sup>C nuclear spins through their chemical bonds leads to a splitting of their resonance peak into two lines (J-coupling) that are separated according to the strength of the interaction. The spectra presented in Figures 2A and 2C show that the acetyl moiety is indeed incorporated into the observed metabolite, as its resonance is split into two lines separated by a frequency corresponding to <sup>13</sup>C–<sup>13</sup>C J-coupling, as is the case for the precursor acetate resonance. This result implies that the acetyl moiety remained intact through the metabolic processes leading to its incorporation into the observed metabolite.

To provide even further evidence for the metabolite assignment, a custom-tailored adiabatic polarization transfer sequence was developed and designed for this particular study.<sup>25</sup> Before

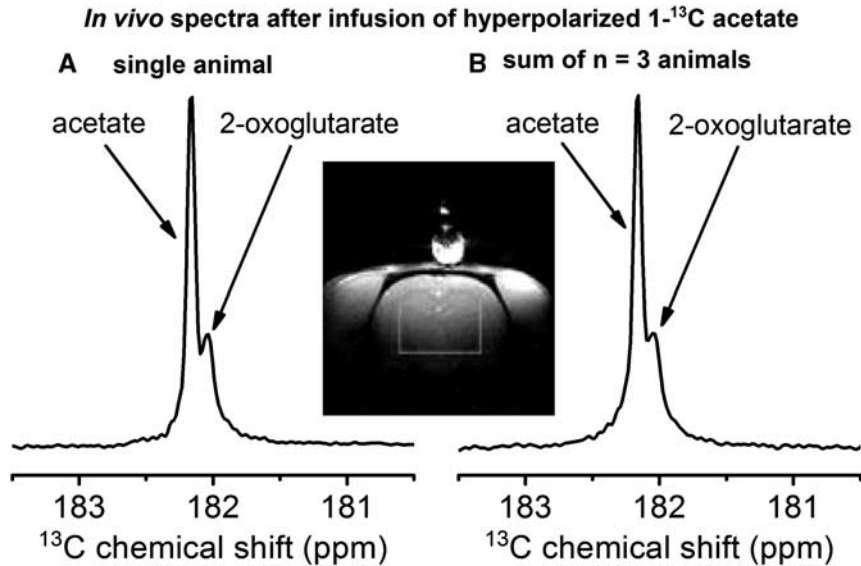


**Figure 1.** *In vivo* localized <sup>13</sup>C spectra measured with a 30° adiabatic pulse applied 4 seconds after the completion of the infusion of hyperpolarized [1-<sup>13</sup>C]acetate. The single scan experiment (**A**) and the sum over three single scan experiments performed in three different animals (**B**) were obtained by selectively detecting the <sup>13</sup>C signal in the area delimited in blue. Please see full text version for color figures.

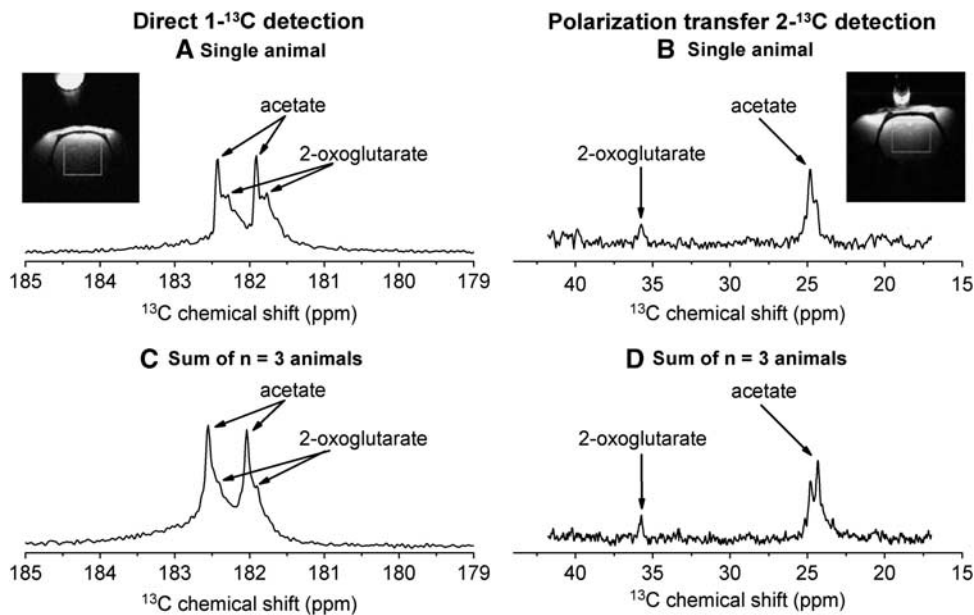


**Figure 2.** (**A, C**) *In vivo* localized <sup>13</sup>C spectra measured with a 30° adiabatic pulse applied 4 seconds after the completion of the infusion of hyperpolarized [1,2-<sup>13</sup>C<sub>2</sub>]acetate. The single scan experiment (**A**) and the sum over three single scan experiments performed in three different animals (**C**) were obtained by selectively detecting the <sup>13</sup>C signal in the area delimited in blue. (**B, D**) *In vivo* localized <sup>13</sup>C spectra measured with a 90° adiabatic pulse applied 4 seconds after the completion of the infusion of [1,2-<sup>13</sup>C<sub>2</sub>]acetate and after carbon-carbon polarization transfer. The single scan experiment (**B**) and the sum over three single scan experiments performed in three different animals (**D**) were obtained by selectively detecting the <sup>13</sup>C signal in the area delimited in blue. Please see full text version for color figures.

detection, the enhanced carboxyl <sup>13</sup>C polarization was transferred to the aliphatic <sup>13</sup>C spins, which exhibit large chemical shift dispersion. Although both the carboxyl and the aliphatic <sup>13</sup>C polarizations are enhanced through DNP, the aliphatic <sup>13</sup>C will not remain hyperpolarized *in vivo* because of its short *T*<sub>1</sub> relaxation time on the order of 2 seconds. This was verified in three experiments, in which no [2-<sup>13</sup>C]acetate signal was observable before polarization transfer. To ensure that the same stage of the metabolic process was probed, the time interval between

dissolution and data acquisition was set as in the previous measurement to 16 seconds. The spectra recorded in the aliphatic region after the polarization transfer are presented in Figures 2B and 2D. The two resonances observed were assigned to acetate (24.5 p.p.m.) and 2OG (36.0 p.p.m.), which is consistent with the carboxyl spectra (Figures 2A and 2C). From the results described above, we conclude that the metabolite observed in the brain after the injection of hyperpolarized acetate is indeed 2OG.

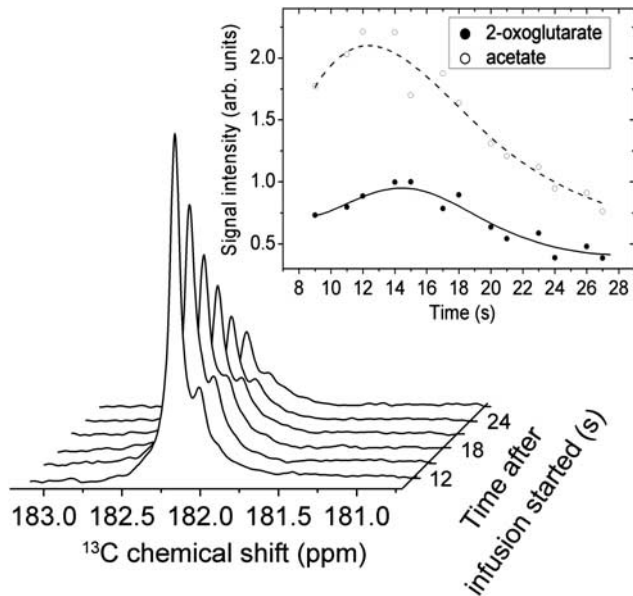


**Figure 3.** Time evolution of the acetate and 2-oxoglutarate (2OG) signal integrals. The spectra shown in the main figure were measured in a single experiment with a series of 30° adiabatic pulse applied every 3 seconds starting after the completion of the infusion. The signal-to-noise ratio of the maximum 2OG was  $25 \pm 5$ . The average ratio between the acetate and the 2OG signal integrals over the entire measurement time was deduced to be  $2.2 \pm 0.3$  in all four experiments using the JMRI software.<sup>44</sup> The open and full circles correspond to the average values of the normalized signal integrals measured in four different animals. The continuous and dotted lines are only drawn as a guide for the eyes and are not deduced from a fit to a model.

The time evolution of the acetate and 2OG signal integrals (data measured on four different animals) is presented in Figure 3. We observed that the maximum signal of 2OG is delayed by  $2 \pm 0.5$  seconds as compared with the maximum signal of acetate. Note that the small ratio between acetate and 2OG signals ( $2.2 \pm 0.3$ ) suggests that the concentration of [1-<sup>13</sup>C]acetate inside the brain is low at the time of the measurements.

## DISCUSSION

To the best of our knowledge, this is the first time 2OG is directly observed *in vivo* in brain. We are not aware of any report describing the detection of 2OG using non-hyperpolarized MR including our own attempts, which implies either an upper concentration limit on the order of  $0.1 \mu\text{mol/g}$  (MR detection limit) or that the intermediate is predominantly in a bound state characterized by a broad and thus unobservable MR signal. Indeed, based on recent structural investigations noting a close colocalization of the TCA cycle enzymes, the proposal has emerged that some, if not all, TCA cycle enzymes may operate *in vivo* as a single unit (metabolon).<sup>28–30</sup> The present study shows that at least a sizable portion of 2OG (an estimation is given below) is sufficiently mobile to be detected by dissolution DNP MR. From recent results on acetate transport in the rat brain reporting Michaelis–Menten parameters,  $V_{max} \sim 1 \mu\text{mol/g/min}$  and  $K_M = \sim 4 \text{mmol/L}$  in the study by Deelchand *et al*<sup>9</sup> or  $V_{max} \sim 1.3 \mu\text{mol/g/min}$  and  $K_M = \sim 27 \text{mmol/L}$  in the study by Patel *et al*,<sup>10</sup> we can estimate that the acetate concentration 20 seconds after the injection is on the order of 0.28 or  $0.19 \mu\text{mol/g}$ , respectively. The average ratio of  $2.2 \pm 0.3$  between the [1-<sup>13</sup>C]acetate and [5-<sup>13</sup>C]2OG signal integrals measured in the

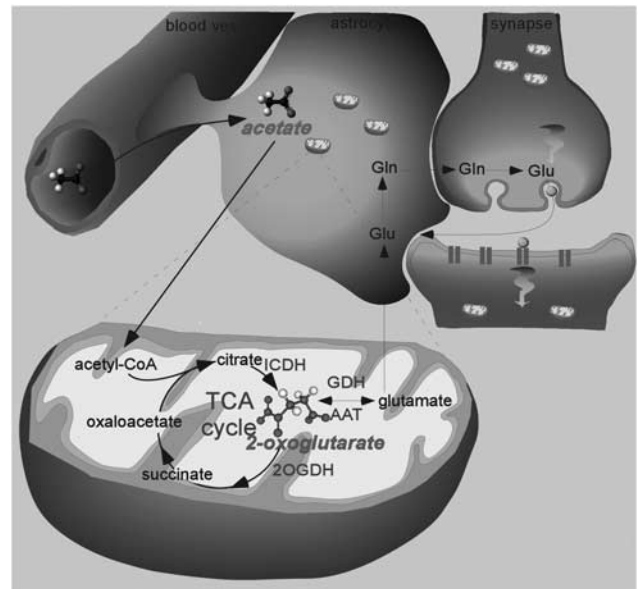


**Figure 4.** Sketch of the glial metabolic processes involving the infused hyperpolarized acetate molecules. The acetate molecules diffuse in the brain and are taken up by the astrocytes before being metabolized in the mitochondria, leading to the creation of 2-oxoglutarate (2OG) through the tricarboxylic acid (TCA) cycle. The chemical structure of the observed hyperpolarized molecules is drawn and their names are highlighted in red. Please see full text version for color figures.

present study (Figure 3) thus suggest that the 2OG concentration in the brain is between  $0.28/2.2 = 0.125 \mu\text{mol/g}$  and  $0.19/2.2 = 0.085 \mu\text{mol/g}$ , which is comparable with the values given by Siesjö.<sup>31</sup> In fact, as 2OG participates in at least three distinct mitochondrial reactions, namely, 2OG dehydrogenase, glutamate dehydrogenase, and AAT, it is unlikely that all enzymes can simultaneously bind to 2OG. We further conclude that as the enhanced polarization must be preserved during the four enzymatic steps between acetyl-CoA and 2OG (Figure 4), all other TCA cycle intermediates, in particular glial citrate, are present at either a much lower concentration than 2OG or in a predominantly bound state.

The <sup>13</sup>C label transfer from mitochondrial TCA cycle intermediate to cytosolic amino acid, in particular Glu, is mediated at least in part by the malate-aspartate shuttle thought to operate at the rate of mitochondrial AAT.<sup>7</sup> Assuming rapid mitochondrial AAT action in astrocytes, one would expect to observe a significant Glu signal. Indeed, assuming a glial Glu concentration of  $\sim 1 \mu\text{mol/g}$  and taking a reported transamination rate of  $\sim 50 \mu\text{mol/g/min}$ ,<sup>7</sup> the turnover time of Glu should be on the order of 1 seconds, which is significantly shorter than the [1-<sup>13</sup>C]Glu T<sub>1</sub> ( $\sim 17$  seconds in perfused heart).<sup>32</sup> It has, however, been suggested that the Glu-aspartate antiporter, known to be rate-limiting for malate-aspartate shuttle, may operate at much lower rates, close to those of the TCA cycle.<sup>5</sup> The absence of Glu signal indeed indicates a slow exchange of label between 2OG and Glu, whether mediated by AAT alone or malate-aspartate shuttle. Assuming a linear fractional enrichment of 2OG from 0% to 100% within the 20 seconds of the experiment, we deduced that the maximum concentration of [5-<sup>13</sup>C]Glu after 20 seconds is given by the integration over time of  $t/20 \cdot V_x \mu\text{mol/g}$  between  $t=0$  and  $t=20$  seconds, where  $V_x$  is the transmembrane label exchange (the dilution of 2OG by the Glu pool is not taken into account). Taking  $V_x = 0.17 \pm 0.01 \mu\text{mol/g/min}$ ,<sup>33</sup> we deduce that the [5-<sup>13</sup>C]Glu concentration should be at most  $0.028 \pm 0.003 \mu\text{mol/g}$ , which seems to be below our detection level as no significant Glu

signal could be observed even after averaging the signals (Figures 1B, 2C and 2D). The fact that citrate was not observed implies that the glial citrate concentration is very low or too broad to be detected. It is of interest to note that recent studies have suggested a very low expression of the Glu-aspartate antiporter in astrocytes.<sup>34</sup>

We conclude from the novel observation of 2OG signal and the lack of Glu signal that the reactions leading to <sup>13</sup>C-label incorporation into Glu are operating, in the glial compartment *in vivo*, at a rate much lower than that of transaminase, thus implying that transport across the inner mitochondria membrane is rate limiting. More generally, the present study illustrates the potential of hyperpolarized acetate as a precursor to non-invasively directly probe glial TCA cycle activity and thus detect pathological alterations hitherto inaccessible to direct observation. The direct determination of TCA cycle intermediates bears the potential to determine TCA cycle rate without the need to assess the conversion and transport of 2OG to glutamate. Several previous *in vivo* studies showed that the hyperpolarized state of <sup>13</sup>C-labels survives metabolic reactions.<sup>35–38</sup> Here, we note that the <sup>13</sup>C polarization is still largely enhanced after as many as four enzymatic reaction steps. Marjańska *et al*<sup>39</sup> did not observe 2OG in the rat brain after the injection of hyperpolarized [2-<sup>13</sup>C]pyruvate, which may be because of the additional reactions implicated, for example, flux through pyruvate dehydrogenase, or to slow transport.

These results show the feasibility of probing the real-time kinetics of the transformation of a fuel into a TCA cycle intermediate *in vivo* in the brain. Recent progress showed that the ability of probing real-time metabolism *in vivo* could become crucial in cancer research.<sup>35,38</sup> In the context of the present study, it is of particular interest to note that a large fraction of gliomas, the most common brain tumor type in humans, are associated with genetic mutations in the isocitrate dehydrogenase enzyme affecting the metabolism of isocitrate and giving the enzyme the ability to produce 2-hydroxyglutarate.<sup>40,41</sup> As the metabolic flux from acetate to 2OG should be affected by variations in the conversion rate between isocitrate and 2OG, the new hyperpolarized MR protocol presented in this report could potentially be used to detect *in vivo* effect of the mutations on the metabolic rates. In addition, as a dramatic reduction of the isocitrate dehydrogenase as well as 2OG dehydrogenase activities were observed in numerous brain disorders,<sup>42</sup> in particular in Alzheimer's disease patients,<sup>43</sup> the ability to measure the <sup>13</sup>C labeling of the 2OG pool in real time could give this metabolite the status of a sensitive biomarker for neurological dysfunctions.

## DISCLOSURE/CONFLICT OF INTEREST

The authors declare no conflict of interest.

## REFERENCES

- Roy CS, Sherrington CS. On the regulation of the blood-supply of the brain. *J Physiol* 1890; **11**: 85–108.
- Krebs HA. The history of the tricarboxylic acid cycle. *Perspect Biol Med* 1970; **14**: 154–170.
- Henry PG, Adriany G, Deelchand D, Gruetter R, Marjanska M, Oz G *et al*. *In vivo* <sup>13</sup>C NMR spectroscopy and metabolic modeling in the brain: a practical perspective. *Magn Reson Imaging* 2006; **24**: 527–539.
- Shulman RG, Rothman DL (eds) *Metabolism by In Vivo NMR*. John Wiley & Sons, Ltd: Chichester, UK, 2004.
- Gruetter R, Seaquist ER, Ugurbil K. A mathematical model of compartmentalized neurotransmitter metabolism in the human brain. *Am J Physiol* 2001; **281**: E100–E112.
- Lebon V, Petersen KF, Cline GW, Shen J, Mason GF, Dufour S *et al*. Astroglial contribution to brain energy metabolism in humans revealed by <sup>13</sup>C nuclear magnetic resonance spectroscopy: elucidation of the dominant pathway for

- neurotransmitter glutamate repletion and measurement of astrocytic oxidative metabolism. *J Neurosci* 2002; **22**: 1523–1531.
- Mason GF, Rothman DL, Behar KL, Shulman RG. NMR determination of the TCA cycle rate and alpha-ketoglutarate/glutamate exchange rate in rat brain. *J Cereb Blood Flow Metab* 1992; **12**: 434–447.
- Cerdan S, Kunnecke B, Seelig J. Cerebral metabolism of [1,2-<sup>13</sup>C]acetate as detected by *in vivo* and *in vitro* <sup>13</sup>C NMR. *J Biol Chem* 1990; **265**: 12916–12926.
- Deelchand DK, Shestov AA, Koski DM, Ugurbil K, Henry PG. Acetate transport and utilization in the rat brain. *J Neurochem* 2009; **109**: 46–54.
- Patel AB, De Graaf RA, Rothman DL, Behar KL, Mason GF. Evaluation of cerebral acetate transport and metabolic rates in the rat brain *in vivo* using H-1-[C-13]-NMR. *J Cereb Blood Flow Metab* 2010; **30**: 1200–1213.
- Bluml S, Moreno-Torres A, Shic F, Nguy CH, Ross BD. Tricarboxylic acid cycle of glia in the *in vivo* human brain. *NMR Biomed* 2002; **15**: 1–5.
- Gruetter R, Novotny EJ, Boulware SD, Mason GF, Rothman DL, Shulman GI *et al*. Localized C-13 NMR-spectroscopy in the human brain of amino-acid labeling from D-[1-C-13]glucose. *J Neurochem* 1994; **63**: 1377–1385.
- Sherry AD, Malloy CR. <sup>13</sup>C isotopomer analysis of glutamate: a NMR method to probe metabolic pathways intersecting in the citric acid cycle. In: Berliner LJ, Robitaille P-M (eds) *In Vivo Carbon-13 NMR* vol. 15. Kluwer Academic Publishers: New York, NY, 2002, pp 59–97.
- Comment A, van den Brandt B, Uffmann K, Kurdzesau F, Jannin S, Konter JA *et al*. Design and performance of a DNP prepolarizer coupled to a rodent MRI scanner. *Concepts Magn Reson* 2007; **31B**: 255–269.
- Jannin S, Comment A, Kurdzesau F, Konter JA, Hautle P, van den Brandt B *et al*. A 140 GHz prepolarizer for dissolution dynamic nuclear polarization. *J Chem Phys* 2008; **128**: 241102–1–4.
- Ardenjaer-Larsen JH, Fridlund B, Gram A, Hansson G, Hansson L, Lerche MH *et al*. Increase in signal-to-noise ratio of > 10,000 times in liquid-state NMR. *Proc Natl Acad Sci USA* 2003; **100**: 10158–10163.
- Comment A, Rentsch J, Kurdzesau F, Jannin S, Uffmann K, van Heeswijk RB *et al*. Producing over 100 ml of highly concentrated hyperpolarized solution by means of dissolution DNP. *J Magn Reson* 2008; **194**: 152–155.
- Sano H, Naruse M, Matsumoto K, Oi T, Utsumi H. A new nitroxyl-probe with high retention in the brain and its application for brain imaging. *Free Radical Bio Med* 2000; **28**: 959–969.
- Xiang Y, Shen J. *In vivo* detection of intermediate metabolic products of [1-C-13]ethanol in the brain using C-13 MRS. *NMR Biomed* 2011; **24**: 1054–1062.
- Lee HB, Blaurock MD. Blood volume in the rat. *J Nucl Med* 1985; **26**: 72–76.
- Lien YHH, Shapiro JL, Chan L. Effects of hypernatremia on organic brain osmoles. *J Clin Invest* 1990; **85**: 1427–1435.
- Staewen RS, Johnson AJ, Ross BD, Parrish T, Merkle H, Garwood M. 3-D FLASH imaging using a single surface coil and a new adiabatic pulse, BIR-4. *Invest Radiol* 1990; **25**: 559–567.
- Choi IY, Tkac I, Ugurbil K, Gruetter R. Noninvasive measurements of [1-(13)C]glycogen concentrations and metabolism in rat brain *in vivo*. *J Neurochem* 1999; **73**: 1300–1308.
- Gruetter R, Tkac I. Field mapping without reference scan using asymmetric echo-planar techniques. *Magn Reson Med* 2000; **43**: 319–323.
- Mishkovsky M, Cheng T, Comment A, Gruetter R. Localized *in vivo* hyperpolarization transfer sequences. *Magn Reson Med* 2012; **68**: 349–352.
- Abragam A, Goldman M. Principles of dynamic nuclear-polarization. *Rep Prog Phys* 1978; **41**: 395–467.
- Fan WMT. Metabolite profiling by one- and two-dimensional NMR analysis of complex mixtures. *Prog Nucl Mag Res Sp* 1996; **28**: 161–219.
- Meyer FM, Gerwig J, Hammer E, Herzberg C, Commichau FM, Volker U *et al*. Physical interactions between tricarboxylic acid cycle enzymes in *Bacillus subtilis*: evidence for a metabolon. *Metab Eng* 2011; **13**: 18–27.
- Srere PA. Why Are Enzymes So Big. *Trends Biochem Sci* 1984; **9**: 387–390.
- Welch GR. On the role of organized multienzyme systems in cellular metabolism: a general synthesis. *Prog Biophys Mol Biol* 1977; **32**: 103–191.
- Siesjö BK. *Brain Energy Metabolism*. John Wiley & Sons, Ltd: New York, NY, 1978.
- Schroeder MA, Atherton HJ, Ball DR, Cole MA, Heather LC, Griffin JL *et al*. Real-time assessment of Krebs cycle metabolism using hyperpolarized <sup>13</sup>C magnetic resonance spectroscopy. *FASEB J* 2009; **23**: 2529–2538.
- Lanz B, Xin L, Gruetter R. Improved quantification of mitochondrial exchange, TCA cycle rate and neurotransmission flux using 1H{13C} MRS measurements of C4 and C3 of glutamate and glutamine. *Proc Int Soc Mag Reson Med* 2010; **18**.
- Contreras L, Satrustegui J. Calcium signaling in brain mitochondria: interplay of malate aspartate NADH shuttle and calcium uniporter/mitochondrial dehydrogenase pathways. *J Biol Chem* 2009; **284**: 7091–7099.
- Albers MJ, Bok R, Chen AP, Cunningham CH, Zierhut ML, Zhang VY *et al*. Hyperpolarized <sup>13</sup>C lactate, pyruvate, and alanine: noninvasive biomarkers for prostate cancer detection and grading. *Cancer Res* 2008; **68**: 8607–8615.

- 36 Gallagher FA, Kettunen MI, Day SE, Hu DE, Ardenkjaer-Larsen JH, Zandt R *et al*. Magnetic resonance imaging of pH *in vivo* using hyperpolarized <sup>13</sup>C-labelled bicarbonate. *Nature* 2008; **453**: 940–943.
- 37 Golman K, in't Zandt R, Thaning M. Real-time metabolic imaging. *Proc Natl Acad Sci USA* 2006; **103**: 11270–11275.
- 38 Day SE, Kettunen MI, Gallagher FA, Hu DE, Lerche M, Wolber J *et al*. Detecting tumor response to treatment using hyperpolarized (<sup>13</sup>C) magnetic resonance imaging and spectroscopy. *Nat Med* 2007; **13**: 1382–1387.
- 39 Marjańska M, Iltis I, Shestov AA, Deelchand DK, Nelson C, Ugurbil K *et al*. *In vivo* C-13 spectroscopy in the rat brain using hyperpolarized [1-C-13]pyruvate and [2-C-13]pyruvate. *J Magn Res* 2010; **206**: 210–218.
- 40 Dang L, White DW, Gross S, Bennett BD, Bittinger MA, Driggers EM *et al*. Cancer-associated IDH1 mutations produce 2-hydroxyglutarate. *Nature* 2009; **462**: 739–744.
- 41 Yan H, Parsons DW, Jin G, McLendon R, Rasheed BA, Yuan W *et al*. IDH1 and IDH2 mutations in gliomas. *N Engl J Med* 2009; **360**: 765–773.
- 42 Bubber P, Ke ZJ, Gibson GE. Tricarboxylic acid cycle enzymes following thiamine deficiency. *Neurochem Int* 2004; **45**: 1021–1028.
- 43 Bubber P, Haroutunian V, Fisch G, Blass JP, Gibson GE. Mitochondrial abnormalities in Alzheimer brain: mechanistic implications. *Ann Neurol* 2005; **57**: 695–703.
- 44 Naressi A, Couturier C, Devos JM, Janssen M, Mangeat C, de Beer R *et al*. Java-based graphical user interface for the MRUI quantitation package. *MAGMA* 2001; **12**: 141–152.